Universal two-body-Hamiltonian quantum computing

Daniel Nagaj*

Research Center for Quantum Information, Institute of Physics, Slovak Academy of Sciences, Dúbravská cesta 9, 84215 Bratislava, Slovakia

(Received 22 November 2011; published 27 March 2012)

We present a Hamiltonian quantum-computation scheme universal for quantum computation. Our Hamiltonian is a sum of a polynomial number (in the number of gates L in the quantum circuit) of constant-norm, time-independent, two-body interaction terms. Furthermore, each qubit in the system interacts only with a constant number of other qubits in a three-layer, geometrically local layout. The computer runs in three steps—it starts in a simple initial product state, evolves according to a time-independent Hamiltonian for time of order L^2 (up to logarithmic factors), and finishes with a two-qubit measurement. Our model improves previous universal two-local-Hamiltonian constructions, as it avoids using perturbation gadgets and large energy-penalty terms in the Hamiltonian, which would result in a large required run time.

DOI: 10.1103/PhysRevA.85.032330 PACS number(s): 03.67.Lx, 03.67.Ac

I. INTRODUCTION

Part of today's effort at achieving a realization of a quantum computer is turning away from the traditional quantum-circuit model with sequential application of unitary gates [1]. Instead, measurement-based computation [2], cluster-state quantum computation [3], topological quantum computation [4], computation by quantum walks [5], adiabatic quantum computation (AQC) [6], and the usage of adiabatic gate teleportation [7] are some of the recently explored alternatives.

Universal quantum computation is possible even with restricted control of only a few of the qubits [8]. We can restrict the limitations on time-dependent control even more and use a system with time-independent interactions. Such a Hamiltonian quantum computer (HQC), or ergodic quantum computer [9] runs in three stages. First, it starts in a simple initial computational-basis product state. Second, the system undergoes Schrödinger time evolution for some time. Finally, we measure a few of the qubits in the computational basis to obtain the answer to the computation. However, so far the universal systems involved at least three local (long-range) interactions [10,11], or two-local nearest-neighbor interactions (on a chain) of high-dimensional particles (qudits) [12–14]. Lloyd [15] has shown that the HQC model is universal, not needing even the adiabatically slow change of the interaction strengths seen in [16]. The computer "runs" (as a quantum walk) in an invariant computational subspace, and the relevant excited states of the Hamiltonian also contain the result of the computation.

Until now, the only universal quantum computation model with a two-local qubit Hamiltonian with restricted time control was an AQC model. It relies on slow change of the Hamiltonian, keeping the system in its ground state. The proofs of universality of the AQC [16–18] rely on techniques from Kitaev's Quantum Merlin Arthur (QMA) complete local Hamiltonian problem [19]. The two-local version of this is based on [20,21] (with restricted terms in [22]), with a gap over the ground state lower-bounded by a high-degree inverse polynomial in the circuit size L. The required runtime of this model (to ensure adiabatic evolution) is a high-degree polynomial in L.

We present a universal two-local-Hamiltonian quantum computer construction in the HQC model with a polynomial (in L) number of constant-norm interaction terms. The runtime of this model is now only L^2, and time control of the interactions is not necessary anymore (except for initial product-state preparation). We construct our two-body, qubit Hamiltonian without using perturbation gadgets, by combining the railroad switch [23] and entangled-clock [11] ideas, ensuring that the evolution of a simple initial product state does not leave the computational subspace. Furthermore, there is a possible three-layer layout of our system so that each qubit interacts only with a constant number of spatially local neighbors. Our construction thus increases the list of classes of Hamiltonians that are difficult to simulate on a classical computer. On the other hand, by simplifying the particle dimension, interaction geometry, types, and strengths, we present a model that is getting closer to realistic Hamiltonians, available, e.g., in a superconducting quantum-computing architecture [24].

II. EVOLUTION WITHIN A GOOD SUBSPACE

Consider a quantum circuit $U = U_L U_{L-1} \dots U_2 U_1$ with L at most two-local unitary gates. We would like to obtain the result of U acting on some n-qubit initial state $|\varphi_0\rangle$, i.e., to measure the first (output) qubit of the state $U|\varphi_0\rangle$. Instead of working with just the n "work" qubits of $|\varphi_0\rangle$, we utilize a quantum system with two registers $\mathcal{H}_w \otimes \mathcal{H}_c$, work and clock. The work register holds the work qubits and the clock register contains pointer states corresponding to the progress of the computation. Consider now the "line" of states

$$|\psi_t\rangle = (U_t U_{t-1} \dots U_2 U_1 |\varphi_0\rangle) \otimes |t\rangle_c \qquad (1)$$

for $t = 0, \dots, L$. These states encode the progress of the quantum circuit U acting on the initial state $|\varphi_0\rangle$, and the state $|\psi_L\rangle$ contains the result of the quantum circuit acting on $|\varphi_0\rangle$. Denote the span of these states $\mathcal{H}_{\mathrm{cmp}}^{\varphi_0} = \mathrm{span}\{|\psi_t\rangle\}$ and call it the *computational subspace*. Our approach is to use a system whose Hamiltonian does not induce transitions out of $\mathcal{H}_{\mathrm{cmp}}^{\varphi_0}$. This makes the dynamics of this model and its required running time simple to analyze.

*daniel.nagaj@savba.sk

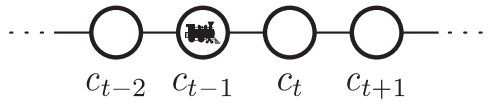

FIG. 1. The pulse clock—a line of $L+1$ qubits c_t with a single active site (train). The states $|t\rangle_c$ are encoded as $|0\dots010\dots0\rangle$, with qubit c_t in the state $|1\rangle$. When the train moves from c_{t-1} to c_t, gate U_t is applied to two work qubits.

We start with Feynman's Hamiltonian [25]:

$$H_F = \sum_{t=1}^{L} \underbrace{(U_t \otimes |t\rangle\langle t-1|_c + U_t^\dagger \otimes |t-1\rangle\langle t|_c)}_{H_F^{(t)}}. \qquad (2)$$

Observe that the computational subspace is invariant under H_F. The restriction of H_F to $\mathcal{H}_{\rm cmp}^{\varphi_0}$ is

$$H_F\big|_{\mathcal{H}_{\rm cmp}^{\varphi_0}} = \sum_{t=1}^{L}(|\psi_t\rangle\langle\psi_{t-1}| + |\psi_{t-1}\rangle\langle\psi_t|), \qquad (3)$$

a quantum walk on the "line" of states $|\psi_t\rangle$. We now use a *pulse clock* encoding $|t\rangle_c = |0\dots0_{c_{t-1}}1_{c_t}0_{c_{t+1}}\dots0\rangle$ of the clock register states, using $L+1$ qubits (see Fig. 1). We can make the terms in the Hamiltonian (2) at most four local, as the gates U_t are at most two local and we can use two-local operators for the clock-register transitions

$$|t\rangle\langle t-1|_c = \mathbb{I}\otimes|01\rangle\langle 10|_{c_{t-1},c_t}\otimes\mathbb{I}. \qquad (4)$$

Writing it like this, we obtain a four-local Hamiltonian different from H_F. However, its restriction to $\mathcal{H}_{\rm cmp}^{\varphi_0}$ is again (3), generating the desired quantum walk on a line starting with the initial state $|\psi_0\rangle = |\varphi_0\rangle|0\rangle_c$. The last step of the HQC model is then to measure the clock register and the output work qubit. If we find the clock register in the state $|L\rangle_c$, we obtain the answer to the computation. We boost the probability to actually measure $|L\rangle_c$ (or in our case, $|1\rangle_{c_L}$) by adding many identity gates at the end of the circuit U. This means that measuring $|1\rangle_{c_{t>L}}$ is enough to ensure the output work qubit holds the output of U, and is thus enough to ensure BQP (bounded-error quantum polynomial-time, i.e. standard quantum computation) universality.

An alternative way of boosting the final probability without extending the clock is to use perfect state-transfer methods [26]. Our desired evolution in the computational basis corresponds to the movement of a single excitation. Using tuned (but still at-most-constant-norm) terms allows us to enforce the progress of a single excitation through the clock register so that it appears perfectly at the other end of a chain at a particular time.

III. THE RAILROAD SWITCH

We now modify the clock register, introducing a *railroad switch* gadget [23,25]. This will give us a three-local Hamiltonian equal to (3) when restricted to the computational subspace. The pulse clock (see Fig. 1) can be viewed as a train running on a single track. When it goes between stations c_{t-1} and c_t, the transition in H_F ensures that the gate U_t is applied to the corresponding work qubits in the work register. The railroad switch (see Fig. 2) introduces four extra stations

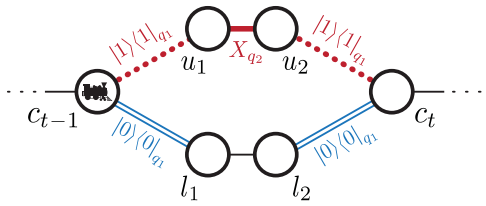

FIG. 2. (Color online) The three-local railroad switch gadget for the application of a controlled-NOT (CNOT) gate between work qubits q_1 and q_2. The state of the control (train master) qubit q_1 in the work register decides whether the train moves to the upper or lower track from c_{t-1} (and backward from c_t). On the upper track, we flip the target work qubit q_2 when the train moves from u_1 to u_2.

between c_{t-1} and c_t, allowing the train to run on two tracks. The train is allowed to move to the upper or lower track depending on the state of a "train master"—one of the work qubits q_1. Furthermore, the target work qubit q_2 is flipped onto the upper track as the train moves from u_1 to u_2. The computational paths running on the upper and lower tracks interfere at station c_t. This gadget facilitates the application of a CNOT gate on the work qubits q_1 and q_2.

Let us look at the dynamics coming from this Hamiltonian. Denote the extra clock states (train positions) between $|t-1\rangle_c$ and $|t\rangle_c$ as $|u_1\rangle_c, |u_2\rangle_c, |l_1\rangle_c, |l_2\rangle_c$. We replace $H_F^{(t)}$ in (2) by

$$\begin{aligned} H_{\rm sw}^{(t)} = {} & |0\rangle\langle 0|_{q_1}\otimes(|l_1\rangle\langle t-1|_c + |t\rangle\langle l_2|_c) \\ & + |1\rangle\langle 1|_{q_1}\otimes(|u_1\rangle\langle t-1|_c + |t\rangle\langle u_2|_c) \\ & + X_{q_2}\otimes|u_2\rangle\langle u_1|_c + \mathbb{I}\otimes|l_2\rangle\langle l_1|_c + \text{c.c.} \end{aligned} \qquad (5)$$

We make all of the terms three local by writing each clock transition such as $|l_1\rangle\langle t-1|_c$ only two-locally as $|01\rangle\langle 10|_{l_1,c_{t-1}}$. Each term in $H_{\rm sw}^{(t)}$ then acts nontrivially on at most one work qubit (q_1 or q_2), and two clock qubits. We now augment the line of states (1), taking into account the intermediary states we introduced. First, write $|\psi_{t-1}\rangle = (|\varphi_{t-1}^{q_1=0}\rangle + |\varphi_{t-1}^{q_1=1}\rangle)\otimes|t-1\rangle_c$ where $|\varphi_{t-1}^{q_1=s}\rangle$ is the part of the work register with the control qubit q_1 in the state $|s\rangle$. Define two extra states between $|\psi_{t-1}\rangle$ and $|\psi_t\rangle$:

$$\begin{aligned} |\psi_t^1\rangle &= |\varphi_{t-1}^{q_1=0}\rangle\otimes|l_1\rangle_c + |\varphi_{t-1}^{q_1=1}\rangle\otimes|u_1\rangle_c, \\ |\psi_t^2\rangle &= |\varphi_{t-1}^{q_1=0}\rangle\otimes|l_2\rangle_c + X_{q_2}|\varphi_{t-1}^{q_1=1}\rangle\otimes|u_2\rangle_c. \end{aligned} \qquad (6)$$

These states are again connected as a line, because $\langle\psi_{t-1}|H_{\rm sw}^{(t)}|\psi_t^1\rangle = \langle\psi_t^1|H_{\rm sw}^{(t)}|\psi_t^2\rangle = \langle\psi_t^2|H_{\rm sw}^{(t)}|\psi_t\rangle = 1$. We now use one railroad switch for every CNOT gate,

$$H_{\rm sw} = \sum_{t:1-{\rm qubit}U_t} H_F^{(t)} + \sum_{\rm CNOT\ gates} H_{\rm sw}^{(t)}, \qquad (7)$$

and augment the subspace $\mathcal{H}_{\rm cmp}^{\varphi_0}$ by the two extra states (6) for each of the gadgets. This results in a three-local Hamiltonian (7), whose restriction to the computational subspace is again (3), generating a quantum walk on the augmented line (1). Note that for the single qubit gates, the operator $U_t\otimes|t\rangle\langle t-1|_c$ is already three local using the original pulse clock encoding.

IV. A QUBIT-QUTRIT SWITCH

If we allow the use of qutrits (e.g., spin-1 particles) in our system, we can decrease the locality of interactions from

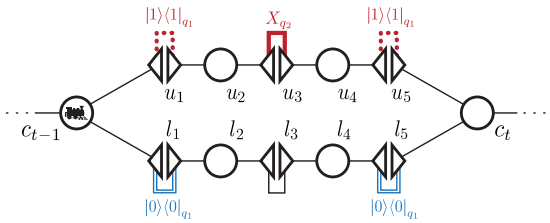

FIG. 3. (Color online) The two-local railroad switch gadget made from qubits (circles) and qutrits (pairs of triangles). The transitions within a qutrit can be controlled by a train master, e.g., the internal transition $|u_{1\mathtt{A}}\rangle_c \leftrightarrow |u_{1\mathtt{B}}\rangle_c$ is allowed only when q_1 is $|1\rangle$. Only on the upper track do we flip the target work qubit q_2 during the internal qutrit transition $|u_{3\mathtt{A}}\rangle_c \leftrightarrow |u_{3\mathtt{B}}\rangle_c$.

three to two body. We build the railroad tracks from qutrits, interspersing them with qubits (so that two qutrits do not interact), setting up the interactions as in Fig. 3. We can view the two states of the clock qubits as an empty station $|0\rangle$, and a train $|1\rangle$ in it. On the other hand, a qutrit station is either empty $|\mathtt{0}\rangle$, or has the train in one of its two stops $|\mathtt{A}\rangle$ or $|\mathtt{B}\rangle$. This allows a two-local interaction to change the state of a work qubit while changing stations within a qutrit. In the three-local railroad switch, the train master work qubit q_1 decided whether the train could pass to the upper or lower track (see Fig. 2). Here, the controlled transitions happen between the internal stops of the qutrits u_1,u_5,l_1,l_5. In addition, we flip the target work qubit q_2 during the internal transition $|u_{3\mathtt{A}}\rangle_c \leftrightarrow |u_{3\mathtt{B}}\rangle_c$. The Hamiltonian for the upper track (see Fig. 3) is

$$\begin{aligned} H_{23u}^{(t)} &= |u_{1\mathtt{A}}\rangle\langle t-1|_c + |u_{1\mathtt{B}}\rangle\langle u_{1\mathtt{A}}|_c \otimes |1\rangle\langle 1|_{q_1} \\ &\quad + |u_2\rangle\langle u_{1\mathtt{B}}|_c + |u_{3\mathtt{A}}\rangle\langle u_2|_c + |u_{3\mathtt{B}}\rangle\langle u_{3\mathtt{A}}|_c \otimes X_{q_2} \\ &\quad + |u_4\rangle\langle u_{3\mathtt{B}}|_c + |u_{5\mathtt{A}}\rangle\langle u_4|_c + |u_{5\mathtt{B}}\rangle\langle u_{5\mathtt{A}}|_c \otimes |1\rangle\langle 1|_{q_1} \\ &\quad + |t\rangle\langle u_{5\mathtt{B}}|_c + \text{c.c.}, \end{aligned} \tag{8}$$

where $\{|u_{1\mathtt{A}}\rangle_c, |u_{1\mathtt{B}}\rangle_c, \dots\}$ are the clock register states corresponding to the eight possible positions of the train on the upper track. When the clock register has a single train in it, we can identify the clock states one-locally (e.g., $|u_{1\mathtt{B}}\rangle\langle u_{1\mathtt{B}}|_c = |\mathtt{B}\rangle\langle\mathtt{B}|_{u_1}$). The transition operators (e.g., $|u_{3\mathtt{A}}\rangle\langle u_2|_c = |\mathtt{0A}\rangle\langle\mathtt{10}|_{u_2,u_3}$) can thus be implemented two-locally. Moreover, the operators involving a work qubit (e.g., $|u_{5\mathtt{B}}\rangle\langle u_{5\mathtt{A}}|_c \otimes |1\rangle\langle 1|_{q_1} = |\mathtt{B}\rangle\langle\mathtt{A}|_{u_5} \otimes |1\rangle\langle 1|_{q_1}$) can also be made two local. Therefore, all the terms in $H_{23t}^{(t)}$ are two local, involving at most one qubit and one qutrit. The Hamiltonian $H_{23l}^{(t)}$ for the lower track is analogous to (8), with corresponding lower-track clock states $\{|l_{1\mathtt{A}}\rangle_c, \dots\}$ and a simple term $|l_{3\mathtt{B}}\rangle\langle l_{3\mathtt{A}}|_c$ (without flipping q_2). Now replace each three-local switch $H_{\mathrm{sw}}^{(t)}$ (5) with

$$H_{23}^{(t)} = H_{23u}^{(t)} + H_{23l}^{(t)}. \tag{9}$$

The basis of the computational subspace $\mathcal{H}_{\mathrm{cmp}}^{\varphi_0}$ again needs to be augmented, similarly to what we did in (6). After $|\psi_{t-1}\rangle$, we write the eight states

$$\begin{aligned} |\psi_t^r\rangle &= |\varphi_{t-1}^{q_1=0}\rangle \otimes |l_r\rangle_c + |\varphi_{t-1}^{q_1=1}\rangle \otimes |u_r\rangle_c, \\ |\psi_t^s\rangle &= |\varphi_{t-1}^{q_1=0}\rangle \otimes |l_s\rangle_c + X_{q_2}|\varphi_{t-1}^{q_1=1}\rangle \otimes |u_s\rangle_c, \end{aligned} \tag{10}$$

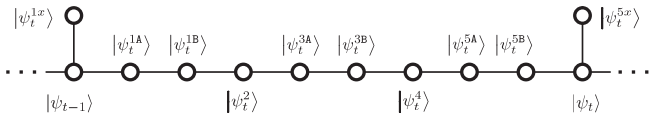

FIG. 4. The geometry of the connections of the computational basis states (10) and (11) implied by the transitions in the Hamiltonian (9) for the qubit-qutrit two-local railroad switch.

with $r \in \{1\mathtt{A}, 1\mathtt{B}, 2, 3\mathtt{A}\}$ and $s \in \{3\mathtt{B}, 4, 5\mathtt{A}, 5\mathtt{B}\}$. Moreover, we have the two "blind-alley" states, with the train trying to use the track where it does not belong,

$$\begin{aligned} |\psi_t^{1x}\rangle &= |\varphi_{t-1}^{q_1=0}\rangle \otimes |u_{1\mathtt{A}}\rangle_c + |\varphi_{t-1}^{q_1=1}\rangle \otimes |l_{1\mathtt{A}}\rangle_c, \\ |\psi_t^{5x}\rangle &= |\varphi_{t-1}^{q_1=0}\rangle \otimes |u_{5\mathtt{A}}\rangle_c + X_{q_2}|\varphi_{t-1}^{q_1=1}\rangle \otimes |l_{5\mathtt{A}}\rangle_c. \end{aligned} \tag{11}$$

The Hamiltonian (9) connects these states with transitions whose geometry is depicted in Fig. 4. It is a line as we have seen before, with the two blind-alley states (11). The quantum-walk dynamics induced on this graph is again similar to the quantum walk on a line, with mixing time (in the time-averaged sense) on the order of $O(L^2)$ for a convergence parameter choice $\epsilon = L^{-1}$, up to logarithmic factors [27].

The crucial fact about this construction is the restriction of the computation to the computational subspace. Problematic states coming from the wrong initial state, states with more than one (or simply no) trains, and bound states on the insides of the "wrong" tracks are not contained in $\mathcal{H}_{\mathrm{cmp}}^{|\varphi_0\rangle}$, making our life much easier.

V. A QUTRIT FROM TWO QUBITS

Finally, we take the qubit-qutrit two-local gadgets and construct the two-local qubit-qubit Hamiltonian using an entangled encoding of clock states similar to the one in [11]. We map the states of the qutrit into states of two qubits as

$$\begin{aligned} |\mathtt{0}\rangle &\rightarrow |00\rangle, \\ |\mathtt{A}\rangle &\rightarrow |+\rangle = \frac{1}{\sqrt{2}}(|01\rangle + |10\rangle), \\ |\mathtt{B}\rangle &\rightarrow |-\rangle = \frac{1}{\sqrt{2}}(|01\rangle - |10\rangle). \end{aligned} \tag{12}$$

Instead of the two-local qutrit-qubit operators of the form $(|\mathtt{B}\rangle\langle\mathtt{A}| + |\mathtt{A}\rangle\langle\mathtt{B}|) \otimes V_d$, we now use

$$\tfrac{1}{2}(Z_1 - Z_2) \otimes V_d, \tag{13}$$

made of two two-local qubit-qubit terms. Here Z_1 and Z_2 act on the two clock qubits encoding the qutrit, and V_d acts on a work qubit. This operator annihilates states of the form $|00\rangle|\varphi\rangle$ and $|11\rangle|\varphi\rangle$, while inducing a transition $|+\rangle|\varphi\rangle \leftrightarrow |-\rangle(V_d|\varphi\rangle)$ using two-qubit entangled clock states $|+\rangle$ and $|-\rangle$. In the Hamiltonian H_{23}, the active qutrit states also appear in the transitions such as $|1\rangle_{c_{t-1}}|\mathtt{0}\rangle_{u_1} \leftrightarrow |0\rangle_{c_{t-1}}|\mathtt{A}\rangle_{u_1}$. Here, this particular transition becomes $|1\rangle_{c_{t-1}}|00\rangle_{u_1,u_1'} \leftrightarrow |0\rangle_{c_{t-1}}|+\rangle_{u_1,u_1'}$,

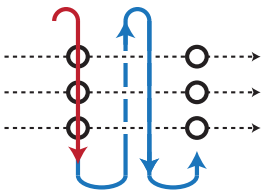

FIG. 5. (Color online) The geometrically local layout of our system. Each column represents n work qubits; the full line depicts the clock register. As the clock progresses, first the gates are applied, and then the column of work qubits is swapped with the next one using CNOT gates, pushing the data to the right. Each qubit is involved in a constant number of two-local interactions. The required number of work qubits is nL.

and is implemented by

$$H_{0+}^{100} = \frac{1}{\sqrt{2}}|0\rangle\langle 1|_{c_{t-1}} \otimes (|1\rangle\langle 0|_{u_1} + |1\rangle\langle 0|_{u_1'}) + \frac{1}{\sqrt{2}}|1\rangle\langle 0|_{c_{t-1}} \otimes (|0\rangle\langle 1|_{u_1} + |0\rangle\langle 1|_{u_1'}), \quad (14)$$

a Hamiltonian built from two-local terms. Note that the states $|0\rangle|00\rangle$ and $|0\rangle|-\rangle$ are annihilated by it. Similarly, we write a Hamiltonian H_{-0}^{001} wherever the transition $|00\rangle|1\rangle \leftrightarrow |-\rangle|0\rangle$ is called for in the clock register. Restricting ourselves to the computational subspace with a single train, this new qubit-qubit two-local Hamiltonian works just like the qubit-qutrit Hamiltonian (9).

The last necessary ingredients in the construction are single-qubit unitaries $W = |w_0\rangle\langle w_0| + e^{i\theta_w}|w_1\rangle\langle w_1|$ which are not self-adjoint. Let the target qubit be the train master, allowing the $|w_1\rangle$ branch on the upper track and $|w_0\rangle$ on the lower track. To make things simpler, we now use a simple pulse-clock encoding of the qutrit u_3 into two qubits $u_{3\mathrm{A}}$ and $u_{3\mathrm{B}}$ on the upper track (and similarly on the lower track). In the middle of the upper track, we then write a two-local interaction term

$$H_{w_1} = (e^{i\theta_w}|01\rangle\langle 10| + e^{-i\theta_w}|10\rangle\langle 01|)_{u_{3\mathrm{A}},u_{3\mathrm{B}}} \quad (15)$$

for the two clock qubits $u_{3\mathrm{A}}$ and $u_{3\mathrm{B}}$. On the lower track, we use $(|01\rangle\langle 10| + |10\rangle\langle 01|)_{l_{3\mathrm{A}},l_{3\mathrm{B}}}$ without the phase shift. The split into two tracks thus allows us to add a relative phase between them which applies the single-qubit gate W to the control work qubit as the computational paths rejoin. The underlying unitary evolution in the computational subspace then again remains equivalent to the one induced by (9).

Finally, we can get geometric locality for this construction. The solution is to use nL work qubits instead of only n, as in Fig. 5, and wrap the clock register around them four times per n work qubits, which is reminiscent of [21]. The winding (in three dimensions) is there to implement a round of gates, and then to perform a swap of a work qubit column with a column of ancillas using two CNOT gates. The data thus move to the next column, and the process continues. Each work qubit interacts with at most five switches, in some of them as a control and in some as a target. Altogether, it is involved in at most 28 two-local qubit-qubit interactions. This is far away from practical, but nevertheless a constant number of interactions per particle.

VI. CONCLUSIONS

We presented a universal two-body-Hamiltonian quantum computer for a three-layer qubit layout, running in three steps: a simple product-state initialization, evolution for a time $O(L^2)$ (up to logarithmic factors) without time-control requirements, and a computational basis measurement checking whether the clock register is in a state $|t > L\rangle_c$. The state of an output work qubit then contains the result of the quantum circuit U acting on the work register of our initial state. Furthermore, our two-body interactions are also spatially local, with a three-layer layout of length $O(L)$ and width $O(n)$, where n is the number of qubits and L the number of gates in the preprocessed circuit.

Although the improvement over previous work might look only incremental at first sight, it is far from straightforward. Before, reduction of a three-body to a two-body requirement on interactions (between qubits) for similar constructions was possible only by utilizing effective Hamiltonians made from two-local terms with large norm, arranged in *perturbation gadgets*. After rescaling, these implied a tiny (although still inverse-polynomial) gap in the Hamiltonian, a large run time, and strict noise-level requirements (if used in an AQC). Our Hamiltonian is spatially local, built from $O(nL)$ constant-norm terms In contrast to previous constructions, our computation scheme based on railroad switches is polynomially faster. The initial product state evolves within a computational subspace, and the evolution is described by a rapidly mixing, continuous-time quantum walk on a necklacelike graph. Moreover, the interaction types utilized here (X,Z,ZZ,XX,ZX,YY) are getting closer to the actual set of interactions (X,Z,ZZ,XX,ZX) available, e.g., in superconducting QC architecture [24]. In conclusion, the class of two-body Hamiltonians presented here (corresponding to different unitary circuits U) is universal for BQP problems and difficult for simulation on a classical computer.

ACKNOWLEDGMENTS

The authors would like to thank the organizers of the ESI workshop Entanglement and Correlations in Many-Body Quantum Mechanics for their hospitality. We want to thank A. Landahl, S. Jordan, A. Lutomirski, D. Gosset, and S. Lloyd for fruitful discussions, an anonymous referee for useful comments, and we gratefully acknowledge support from the EU project Q-ESSENCE and the Slovak Research and Development Agency under the APVV Contract No. LPP-0430-09 and the meta-QUTE ITMS Project No. 26240120022.

[1] M. A. Nielsen and I. L. Chuang, *Quantum Information and Computation* (Cambridge University Press, Cambridge, UK, 2000).

[2] A. M. Childs, D. W. Leung, and M. A. Nielsen, Phys. Rev. A **71**, 032318 (2005).

[3] R. Raussendorf, and H. J. Briegel Phys. Rev. Lett. **86**, 5188 (2001).
[4] A. Yu and Kitaev, Ann. Phys. (NY) **303**, 2 (2003).
[5] A. M. Childs, Phys. Rev. Lett. **102**, 180501 (2009).
[6] E. Farhi *et al*., Science **292**, 472 (2001).
[7] D. Bacon and S. T. Flammia, Phys. Rev. Lett. **103**, 120504 (2009).
[8] A. Kay and P. J. Pemberton-Ross, Phys. Rev. A **81**, 010301(R) (2010); D. Burgarth *et al*., *ibid*. **81**, 040303(R) (2010).
[9] D. Janzing and P. Wocjan, Quantum Inf. Process. **4**, 129 (2005).
[10] S. Bravyi, e-print arXiv:quant-ph/0602108.
[11] D. Nagaj and S. Mozes, J. Math. Phys. **48**, 2104 (2007).
[12] D. Aharonov, D. Gottesman, S. Irani, and J. Kempe, in *Proceedings of the 48th Annual IEEE Symposium on the Foundations of Computer Science* (IEEE Computer Society, Los Alamitos, CA, 2007), pp. 373–383.
[13] D. Nagaj and P. Wocjan, Phys. Rev. A **78**, 032311 (2008); K. G. H. Vollbrecht and J. I. Cirac, Phys. Rev. Lett. **100**, 010501 (2008); B. Chase and A. Landahl, e-print arXiv:0802.1207; A. Kay, Phys. Rev. A **78**, 012346 (2008).
[14] L. Eldar and O. Regev, in *Proceedings of the International Colloquium on Automata, Languages and Programming 2008*, edited by L. Aceto *et al*., Lecture Notes in Computer Science No. 5125 (Springer-Verlag, Berlin, 2008), Part I, pp. 881–892; L. Eldar, P. Love, D. Nagaj, and O. Regev (unpublished).
[15] S. Lloyd, e-print arXiv:0805.2757.
[16] D. Aharonov, W. van Dam, J. Kempe, Z. Landau, S. Lloyd, and O. Regev, SIAM J. Comput. **37**, 166 (2007).
[17] J. Kempe, A. Kitaev, and O. Regev, SIAM J. Comput. **35**, 1070 (2006).
[18] A. Mizel, D. A. Lidar, and M. Mitchell, Phys. Rev. Lett. **99**, 070502 (2008).
[19] A. Y. Kitaev, A. H. Shen, and M. N. Vyalyi, *Classical and Quantum Computation*, Graduate Studies in Mathematics, Vol. 47 (AMS, Providence, RI, 2002).
[20] J. Kempe, A. Kitaev, and O. Regev, in *Proceedings of the 24th Annual Conference on Foundations of Software Technology and Theoretical Computer Science,* Lecture Notes in Computer Science, Vol. 3328, edited by K. Lodaya and M. Mahajan, (Springer, 2004), pp. 372–383.
[21] R. Oliveira and B. M. Terhal, Quantum Inf. Comput. **8**, 900 (2008).
[22] J. D. Biamonte and P. J. Love, Phys. Rev. A **78**, 012352 (2008).
[23] D. Nagaj, J. Math. Phys. **51**, 062201 (2010).
[24] M. Grajcar *et al*., Phys. Rev. B **71**, 144501 (2005).
[25] R. Feynman, Opt. News **11**, 11 (1985); D. de Falco and D. Tamascelli, J. Phys. A **37**, 909 (2004).
[26] A. Kay, Int. J. Quantum Inf. **8**, 641 (2010).
[27] M. Kieferová and D. Nagaj, to appear in Int. J. Quantum Inf. (2012), arXiv:1111.4433.